Journal of South American Earth Sciences 102 (2020) 102672

Contents lists available at ScienceDirect

Journal of South American Earth Sciences

journal homepage: www.elsevier.com/locate/jsames

Upper crustal differentiation processes and their role in 238U-230Th disequilibria at the San Pedro-Linzor volcanic chain (Central Andes)

Benigno Godoy[a,*], Lucy McGee[b,1], Osvaldo González-Maurel[c,d], Inés Rodríguez[e], Petrus le Roux[d], Diego Morata[a], Andrew Menzies[f]

[a] Centro de Excelencia en Geotermia de los Andes (CEGA) y Departamento de Geología, Facultad de Ciencias Físicas y Matemáticas, Universidad de Chile, Plaza Ercilla 803, Santiago, Chile
[b] Department of Earth and Planetary Sciences, Macquarie University, Sydney, NSW, 2109, Australia
[c] Departamento de Ciencias Geológicas, Universidad Católica del Norte, Avda. Angamos, 0610, Antofagasta, Chile
[d] Department of Geological Sciences, University of Cape Town, Rondebosch, 7700, South Africa
[e] Departamento de Obras Civiles y Geología, Facultad de Ingeniería, Universidad Católica de Temuco, Rudecindo Ortega, 02950, Chile
[f] Bruker Nano GmbH, Am Studio 2D, Berlin 12489, Germany

ARTICLE INFO

Keywords:
U-series disequilibria
San Pedro – Linzor volcanic chain
^{238}U excess
Subduction zone magmatism
Amphibole fractionation

ABSTRACT

U-series data are combined with major and trace element constraints to construct a detailed view of the magmatic system feeding the San Pedro-Linzor volcanic chain, aiding the understanding of how stratovolcanoes in extremely thick arc crust evolve. Lavas from the Quaternary San Pedro-Linzor volcanic chain (Central Andes) have (^{238}U/^{230}Th) ranging from 1.015 to 1.072, with ^{238}U excess even in the less evolved (~57 wt% SiO_2) analyzed lavas. Contrary to well-established trends between fluid mobile elements and ^{238}U excess, $(^{238}U/^{230}Th)_0$ shows no systematic correlation with ratios indicative of fluid-driven melting (e.g. Ba/Hf and K/La). Moreover, the inverse correlation between (^{238}U/^{232}Th) with the amount of slab-derived fluid and the oxidation state of the mantle below Central Andes, which decreases eastwards, suggests that the main control of the ^{238}U excess is not associated with hydration of the mantle wedge. Changes in (^{238}U/^{232}Th) and $(^{230}Th/^{232}Th)_0$ are observed with variations in SiO_2 and CaO + Al_2O_3 contents, and ^{87}Sr/^{86}Sr and Dy/Dy* ratios of the lavas. These changes correspond to increasing (^{238}U/^{232}Th) with decreasing Dy/Dy* and CaO + Al_2O_3 ratios, which is attributed to changes in crystallization of mineralogical phases within magmatic chambers during differentiation. Also, ^{230}Th in-growth is produced during stagnation within magmatic chambers located below the San Pedro-Linzor volcanic chain. Finally, a positive correlation between $(^{230}Th/^{232}Th)_0$ and ^{87}Sr/^{86}Sr indicates an important role of crustal contamination, and of new mafic inputs during evolution of the volcanic chain with time. Our observations suggest that better constraints of all magmatic processes are needed to fully understand the U-series disequilibria recognized for the different volcanic structures developed within subduction-related tectonic environments.

1. Introduction

U-series disequilibria correspond to enrichment or depletion of daughter radionuclides (e.g. ^{230}Th, ^{226}Ra) relative to their radioactive parental isotope (e.g. ^{238}U and ^{230}Th respectively) over their respective half-lives. This disequilibria may be related to a range of magmatic processes, such as the onset of fluid-flux melting, or the fractionation of a significant mineral phase, and can be used to constrain these processes, and determine the timescales over which they occur (Condomines et al., 2003; Peate and Hawkesworth, 2005). In subduction-zones, the use of U-series disequilibria can establish the mantle characteristics of these tectonic environments, commonly associated with addition of slab-derived fluids and the in-growth of daughter isotopes through parental isotope decay (Turner et al., 2003; Huang et al., 2016). In these environments, the extent of disequilibria is also used to determine the different processes related to evolution and timescales of the mantle-generated magmas during their ascent (Condomines et al., 2003; Turner et al., 2003). Few magmas that erupt in arc environments, however, remain primitive due to crustal processing. To establish the behavior of U-series during mantle melting

* Corresponding author.
E-mail address: bgodoy@ing.uchile.cl (B. Godoy).
[1] Present address: Department of Earth Sciences, The University of Adelaide, Adelaide 5005, Australia.

https://doi.org/10.1016/j.jsames.2020.102672
Received 24 January 2020; Received in revised form 8 May 2020; Accepted 27 May 2020
Available online 03 June 2020
0895-9811/

processes it is therefore necessary to understand how the upper crustal processes affect the extent of this disequilibria.

The Central Andes corresponds to a subduction-related magmatic arc developed over a > 60 km thick continental crust (Beck et al., 1996). Primitive magmas at this arc are related to partial melting of peridotite mantle (Davidson et al., 1990; Burns et al., 2020) mainly by hydration from slab-derived fluids (Rosner et al., 2003; Araya-Vargas et al., 2019). However, the initial composition of the mantle-derived magmas is obscured by differentiation, mainly by crustal assimilation, occurring during their ascent to the surface (e.g. Davidson et al., 1990, 1991; Feeley and Davidson, 1994; Matthews et al., 1994; Garrison et al., 2006; Figueroa and Figueroa, 2006; de Silva and Kay, 2018; Burns et al., 2020; González-Maurel et al., 2020).

This work contrasts the effects of the different magmatic processes at upper crustal (< 40 km depth) levels in the control of U-series disequilibria in mantle-derived magmas at subduction-related environments. The main objective of this work is to understand how these processes influence the observed U-series disequilibria in young continental volcanic arcs. To establish this, we focus on the San Pedro-Linzor volcanic chain (Central Andes) using previous evolutionary models to discuss the roles of mineral fractionation and magmatic differentiation regimes in the genesis of this disequilibria. We selected samples from the least evolved products of this volcanic chain which were erupted in the last 270 kyr. These samples correspond to lava flows from Paniri and San Pedro volcano, and the lava flow and the scoria cone that form La Poruña.

2. Geological background

2.1. Main features of the San Pedro-Linzor volcanic chain

The San Pedro-Linzor volcanic chain (21°53′S 68°23′W - 22°09′S 67°58′W) corresponds to a ~65 km long NW-SE trending lineament of volcanic structures which were erupted in the western margin of the Altiplano-Puna Volcanic Complex (*sensu* de Silva, 1989) (Fig. 1). This volcanic chain was built in the last 2 Myr (Godoy et al., 2017), over an exceptionally thick continental crust (> 60 km, Beck et al., 1996), overlying Miocene ignimbrites and sedimentary sequences (Godoy et al., 2017; Sélles and Gardeweg, 2017). The San Pedro-Linzor volcanic chain includes a series of different volcanic products such as lava flows and scoria fragments, which form mainly scoria cones (e.g. La Poruña), stratovolcanoes (e.g. San Pedro and Paniri), and coulee flows (e.g. Chao Dacite) (Fig. 1).

The volcanic products selected for this work correspond to different evolutionary stages of San Pedro and Paniri volcanoes, and from La Poruña scoria cone (Fig. 1). These structures were constructed separately < 270 ka (Fig. 1) (Godoy et al., 2018; González-Maurel et al., 2019a). Following the age criteria from González-Maurel et al. (2019a), samples from San Pedro were divided in Old (> 96 ka) and Young (< 96 ka) stages, whilst samples from Paniri correspond to Laguna (165–250 ka) and Llareta (100–165 ka) units from the New Cone Stage (Godoy et al., 2018). La Poruña represents in turn a short-lived eruption that occurred ca. 100 ka (González-Maurel et al., 2019a). Due to the importance of dating to U-series systematics, age information is discussed in detail in section 3 and summarized in Table S3.

2.2. Petrologic evolution of selected volcanic structures

Geochemical and isotopic characteristics indicate that the upper crustal magmatic evolution of the San Pedro-Linzor volcanic chain is associated, first, to the interaction of primitive magmas with partially molten layers of the crust distributed between 10 and 40 km depth (O'Callaghan and Francis, 1986; Godoy et al., 2014, 2017; González-Maurel et al., 2019b). This is similar to what is recognized in other Central Andean volcanoes (e.g. Davidson et al., 1990; Feeley et al., 1993; Matthews et al., 1994; Taussi et al., 2019), for which the

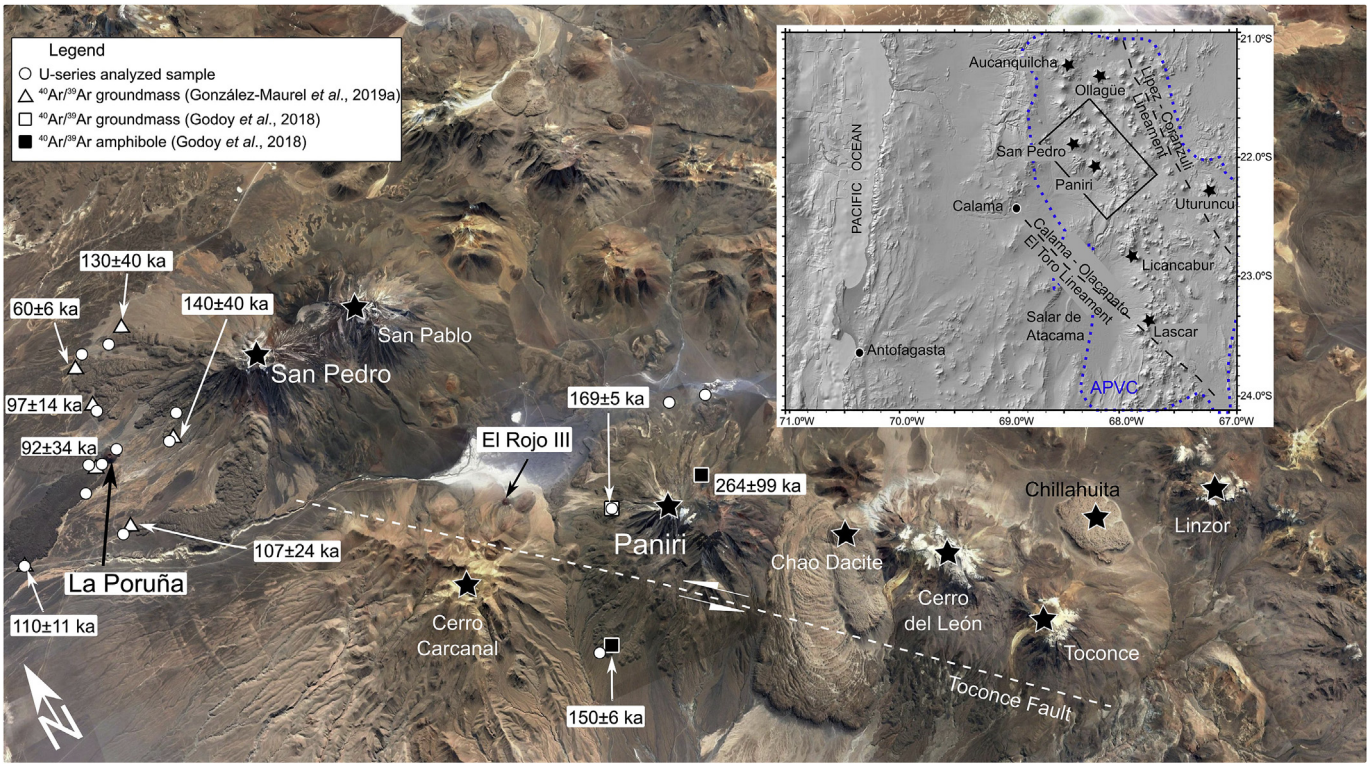

Fig. 1. Satellite image (Google Earth ™) showing location of the San Pedro-Linzor volcanic chain, with ages of the analyzed structures after Godoy et al. (2018) and González-Maurel et al. (2019a). Inset shows location of the volcanic chain, the major volcanic structures in the area between Lipez-Coranzuli and Calama-Olacapato-El Toro lineaments (after Salfity, 1985) and the distribution of the Altiplano-Puna Volcanic Complex (APVC, after de Silva, 1989). Location of Toconce Fault after Giambiagi et al. (2015).

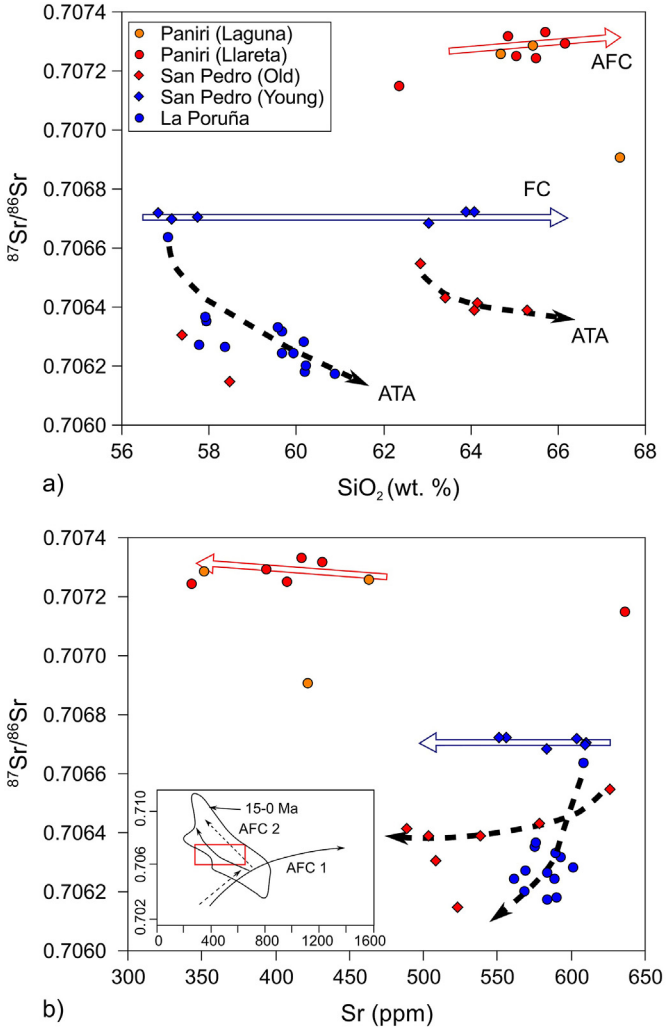

Fig. 2. $^{87}Sr/^{86}Sr$ *versus* SiO_2 (wt.%) (a), and *versus* Sr (ppm) (b) diagrams for the analyzed volcanic structures. In both diagrams assimilation and fractional crystallization (AFC), fractional crystallization (FC), and assimilation during turbulent ascent (ATA) processes are indicated (after Godoy et al., 2014, 2018; and González-Maurel et al., 2019a). The lower contents of isolated data points for samples from San Pedro Old and Paniri are related to recharge processes which lower the crustal assimilation (i.e. $^{87}Sr/^{86}Sr$) signature of the magmas (Godoy et al., 2018; González-Maurel et al., 2019a, b). Star indicates the youngest erupted product of Paniri volcano. Inset in b) is related to the different trends of Central Andean magmatism according to Rogers and Hawkesworth (1989; dashed lines) and Davidson et al. (1990; solid lines).

primitive magmas correspond to mantle-derived melts (e.g. Davidson et al., 1990; González-Maurel et al., 2019a, 2020; Burns et al., 2020) that ascend by exploiting crustal weaknesses (Feeley et al., 1993; Araya-Vargas et al., 2019; González-Maurel et al., 2019a), stagnating at mid-crustal levels (de Silva and Kay, 2018; Godoy et al., 2019). The partially molten layers correspond to the proposed Altiplano-Puna Magma Body (*sensu* Chmielowski et al., 1999), which extends below the Altiplano-Puna Volcanic Complex province (Ward et al., 2014; Kern et al., 2016). This partially molten system is thermally sustained by underplating of primitive magmas (de Silva et al., 2006; González-Maurel et al., 2019b). During the interaction of the primitive magmas and the Altiplano-Puna Magma Body assimilation and fractional crystallization (AFC; *sensu* DePaolo, 1981) is the dominant differentiation process that generates the parental magmas of the San Pedro-Linzor volcanic chain (Godoy et al., 2014, 2017), as suggested for other volcanic products of the Altiplano-Puna Volcanic Complex (e.g. de Silva, 1989; Feeley et al., 1993; Burns et al., 2015; Taussi et al., 2019) (Fig. 2).

A decrease in the percentage of assimilated upper crustal material from the center to the border of the partially molten layer is recognized in the volcanic chain, which is attributed to the decreasing thickness of the Altiplano-Puna Magma Body (Godoy et al., 2017; González-Maurel et al., 2019b).

After this first stage of magmatic evolution, the geochemical and isotopic features link the petrogenesis of each individual structure of the volcanic chain mainly to stagnation of the parental magmas (Godoy et al., 2014; González-Maurel et al., 2019a). This stagnation generates chambers at 4–10 km depth, such as those identified by geophysical data in the area (Kühn et al., 2018; Araya-Vargas et al., 2019; Mancini et al., 2019). In these shallow crustal chambers, petrologic evolution of parental magmas of the San Pedro-Linzor volcanic chain is controlled mainly by fractional crystallization (FC), or by a new stage of AFC which involves small amounts of assimilation of Paleozoic crustal basement (Godoy et al., 2017; González-Maurel et al., 2020), as observed in other volcanoes of the Altiplano-Puna Volcanic Complex (e.g. Feeley et al., 1993; Matthews et al., 1994; Figueroa and Figueroa, 2006; Taussi et al., 2019). In detail, a FC (fractional crystallization) process is recognized in the youngest stage of San Pedro volcano (i.e. San Pedro Young; González-Maurel et al., 2019a), whilst an AFC process is observed at the youngest stages of Paniri volcano (Godoy et al., 2018) (Fig. 2). Moreover, evolution in these shallow crustal magma chambers also includes small degrees of new inputs of primitive magmas (i.e. recharge), which decreases the Sr-isotope content of the erupted products (Godoy et al., 2018; González-Maurel et al., 2019a). This recharge is recognized in the youngest products of Paniri volcano and during the Old stage of San Pedro volcano (Fig. 2), and is also proposed for other volcanoes of the Altiplano-Puna Volcanic Complex (Feeley et al., 1993; Matthews et al., 1994). Finally, differentiation processes are suggested to occur with no magma stagnation (i.e. bypassing the Altiplano-Puna Magma Body; González-Maurel et al., 2019b). This is associated with selective contamination of primitive magmas during their ascent (i.e. assimilation during turbulent ascent -ATA-; Huppert and Sparks, 1985). This process is associated with crustal contamination decreasing with increasing differentiation (i.e. silica content) as recognized at La Poruña and the oldest stage of evolution of San Pedro volcano (González-Maurel et al., 2019a) (Fig. 2), as well as for other Central Andean volcanic structures (Maro et al., 2017).

3. Methods

Major and trace elements, and Sr- and Nd-isotopic analysis, and results, were previously published (Godoy et al., 2014, 2018; González-Maurel et al., 2019a). This data is presented as Supplementary Material (Table S1). Full description of analytical methods, procedures, and results and errors of duplicate and standards analysis is given in González-Maurel et al. (2019a,b).

U and Th concentrations and activity ratios (denoted by parentheses; Table S2) were determined on bulk rock powders at the Macquarie University GeoAnalytical facility (MQGA). Approximately 0.3 g of powdered rock was spiked with a ^{236}U-^{229}Th tracer solution and digested in a mixture of concentrated acids (HF-HNO_3) in Teflon beakers at 120 °C for 48 h. After digestion and dilution of the resultant solutions, U and Th were extracted from the rock matrix using 4 ml columns of BioRad AG1-x8 anionic resin, introducing and eluting the samples in 7N HNO_3, and extracting the Th and U fractions in 6N HCl and 0.2N HNO_3, respectively. Uranium and thorium concentrations, determined by isotope dilution, and U-Th isotope ratios were measured separately on a Nu Instrument Multi-Collector ICP-MS at Macquarie University. For U analyses, the New Brunswick Laboratory (NBL) synthetic standards U010 and U005a were used at regular intervals to assess the robustness of instrumental corrections and to monitor drift. For Th analyses, a standard-sample bracketing procedure for each sample analyzed used the Th 'U' standard solution, and a linear tail correction for the ^{232}Th tail on ^{230}Th was applied. Two samples (POR-15-05 and

SPSP-14-01) were duplicated as separate digestions and show good reproducibility in U and Th concentrations and activity ratios (see Table S2). Two separate digestions of TML (Table Mountain Latite) and one digestion of the USGS standard BCR-2 were prepared and analyzed at the same time as the samples. TML (average of the two analyses) was measured as (^{230}Th/^{232}Th) = 1.073 ± 0.006, and (^{238}U/^{232}Th) = 1.070 ± 0.017 which are within error of values reported by *Scott* et al. (2019) [(^{230}Th/^{232}Th) = 1.077 ± 0.006, (^{238}U/^{232}Th) = 1.070 ± 0.045]. BCR-2 was measured as (^{230}Th/^{232}Th) = 0.872 ± 0.005, and (^{238}U/^{232}Th) = 0.878 ± 0.014 [Scott et al. (2019): (^{230}Th/^{232}Th) = 0.879 ± 0.005, (^{238}U/^{232}Th) = 0.877 ± 0.015]. All standard and duplicate data and error are shown in Table S3.

As the lavas are all older than one half-life of ^{230}Th (75 ka), previously published ages are used for isotopic corrections of (^{230}Th/^{232}Th) (given as (^{230}Th/^{232}Th)$_0$) (see Table S2 and Fig. 1 for ages and dating method, and Table S4 for ages and parameters used for error calculations). La Poruña is a monogenetic scoria cone for which several ages has been published (Wörner et al., 2000; Bertín and Amigo, 2019; González-Maurel et al., 2019a), giving a range of eruption ages between 32 and 160 ka. Considering these published ages, and the magmatic evolution of this volcanic structure (González-Maurel et al., 2019a), an age of 100 ka was used to correct the measured (^{230}Th/^{232}Th) for these samples. For San Pedro and Paniri mostly all analyzed samples were corrected using their published ages (Delunel et al., 2016; Sellés and Gardeweg, 2017; Godoy et al., 2017, 2018; Bertín and Amigo, 2019; González-Maurel et al., 2019a), and considering that a detailed volcanic and magmatic evolution has been carried out for these structures (Francis et al., 1974; O'Callaghan and Francis, 1986; Lazcano, 2016; Martínez, 2014; Godoy et al., 2018; Bertín and Amigo, 2019; González-Maurel et al., 2019a). Sample SPSP-16-06 corresponds to the only analyzed lava from San Pedro without geochronological data which is located stratigraphically over the lava flow where sample SPSP-16-08 was collected (140 ± 40 ka) and below where sample SPSP-14-01 was obtained (60 ± 6 ka) (Fig. 1). Considering that this sample corresponds to the younger (< 96 ka) lava suite of San Pedro (i.e. San Pedro Young; González-Maurel et al., 2019a), an age of 90 ka was used to correct the obtained (^{230}Th/^{232}Th) of this sample with an age range between 54 and 180 ka (Table S4). For sample PANI-16-02 from Paniri, an obtained age of 264 ± 99 ka has been published (Godoy et al., 2018). Stratigraphycally, this sample corresponds to the Llareta Unit that was erupted between 100 and 165 ka (Godoy et al., 2018). Thus, an age of 165 ka was used to correct the (^{230}Th/^{232}Th) data, and minimum and maximum ages of 165 and 264 ka were used as errors for this sample considering the obtained geochronolgical data (Fig. 1). For sample PANI-16-03, which corresponds to the only sample from Paniri without geochronological data, a correction age of 100 ka and an error range between 100 and 174 ka were used, as this sample is considered to be the youngest erupted product from Paniri volcano (Godoy et al., 2018).

4. Results

4.1. Petrographic characteristics

A brief review of the petrographic features of analyzed units is shown in Fig. 3. The mineralogical assemblage of the samples of La Poruña (Fig. 3a–b) consists of phenocrysts (10–30 vol%) of plagioclase, olivine, orthopyroxene and clinopyroxene, with minor amphibole, magnetite and ilmenite. The groundmass is composed of glass, with variable amounts of microlites of the same mineralogical phases (Fig. 3a). Samples from the cone of La Poruña show high vesicularity (up. to 40% vol.) whilst those from the lava flow are highly crystalline (Fig. 3a and b) (Marín et al., 2015; Marín, 2016; Gallmeyer, 2018; Godoy et al., 2019; González-Maurel et al., 2019a,b). Samples from San Pedro volcano are porphyritic (15 to ca. 40 vol% phenocrysts) lava flows (Fig. 3 c-f), consistent with previous observations of O'Callaghan and Francis (1986), and González-Maurel et al. (2019a,b). The mineralogical assemblage was divided into olivine-pyroxene-bearing, and amphibole-bearing (*sensu* González-Maurel et al., 2019a). Olivine-pyroxene-bearing lavas are constituted mainly of phenocrysts of plagioclase + olivine + orthopyroxene ± clinopyroxene, with small amounts of amphibole + magnetite. Amphibole-bearing lavas are mainly constituted of phenocrysts of plagioclase + amphibole ± magnetite, with minor clinopyroxene ± orthopyroxene phenocrysts. Groundmass on both assemblages are composed of glass with variable proportions of plagioclase ± orthopyroxene ± clinopyroxene ± amphibole ± magnetite. Lavas from San Pedro Young (Fig. 3c–d) are richer in amphibole-bearing assemblages, whilst olivine-pyroxene-bearing lavas are more common in the San Pedro Old lavas (Fig. 3f), as described by González-Maurel et al. (2019a). Lava flows from Laguna and Llareta units of Paniri are petrographically similar (Godoy et al., 2018), showing mainly phenocrysts (20–40 vol%) of plagioclase + clinopyroxene ± orthopyroxene ± amphibole in a groundmass composed of glass and plagioclase (Fig. 3g–i). Small amounts (< 5 vol%) of biotite, ilmenite, apatite and zircon have been identified in lava samples from these units (Martínez, 2014; Lazcano, 2016; Godoy et al., 2018). However, the youngest event of Paniri (ca. 100 ka) generated volcanic products constituted of plagioclase ± orthopyroxene phenocrysts, with microlites of the same mineralogical assemblage (Fig. 3i).

4.2. U-Th activity

The composition of the products of the studied volcanic structures (San Pedro, La Poruña, and Paniri) varies between 56 and 68 wt% SiO_2 (Fig. 2). U-series results show ^{238}U enrichment of the samples with (^{238}U/^{230}Th) ranging from 1.015 to 1.072 (Table S2). Compared with other Andean volcanoes, built over thick continental crust (> 40 km), the San Pedro-Linzor volcanic chain has similar (^{230}Th/^{232}Th)$_0$ and (^{238}U/^{232}Th) to published data from Parinacota (Fig. 4a). La Poruña shows the lowest (^{238}U/^{232}Th) and (^{230}Th/^{232}Th)$_0$, for which both ratios decrease slightly with increasing ^{87}Sr/^{86}Sr (Fig. 4c and d). Lavas of San Pedro Young have similar ^{87}Sr/^{86}Sr, which do not correlate with (^{238}U/^{232}Th) and (^{230}Th/^{232}Th)$_0$. However, an abrupt increase in (^{238}U/^{232}Th) and (^{230}Th/^{232}Th)$_0$ is observed with increasing SiO_2 content of these samples (Fig. 4c and d). For San Pedro Old (^{238}U/^{232}Th) increases, and (^{230}Th/^{232}Th)$_0$ decreases with ^{87}Sr/^{86}Sr (Fig. 4c and d), which is opposite to the differentiation trend of these samples (Fig. 2). Paniri (Llareta and Laguna units) shows the highest (^{238}U/^{232}Th) and (^{230}Th/^{232}Th)$_0$ (Fig. 4b), which correlate positively with ^{87}Sr/^{86}Sr (Fig. 4c and d), with (^{238}U/^{232}Th) increasing abruptly with increasing SiO_2 content (Fig. 4c).

5. Discussion

5.1. Main control of U-series disequilibria at San Pedro-Linzor volcanic chain

As for other Andean volcanoes (e.g. Bourdon et al., 2000; Garrison et al., 2006; Kiebala, 2008) the variation in ^{238}U-^{230}Th disequilibria from the structures of the San Pedro-Linzor volcanic chain reflects either initial source melting processes or subsequent differentiation processes (Turner et al., 2003; Garrison et al., 2006; Huang et al., 2016).

At subduction-related environments, mainly at oceanic arcs, ^{238}U excesses are typically attributed to addition of fluids from the slab to the mantle wedge (Hawkesworth et al., 1997; Turner et al., 2003). This can be constrained with fluid-mobile trace elements (e.g. Ba and K) as indicated by El Misti volcano at the Central Andes (Kiebala, 2008), and the High-Mg basaltic center San Jorge in the Andean Southern Volcanic Zone (McGee et al., 2019). The basalts from San Jorge have large U-excesses and Ra-excesses which correlate with Ba/Hf and K/La ratios.

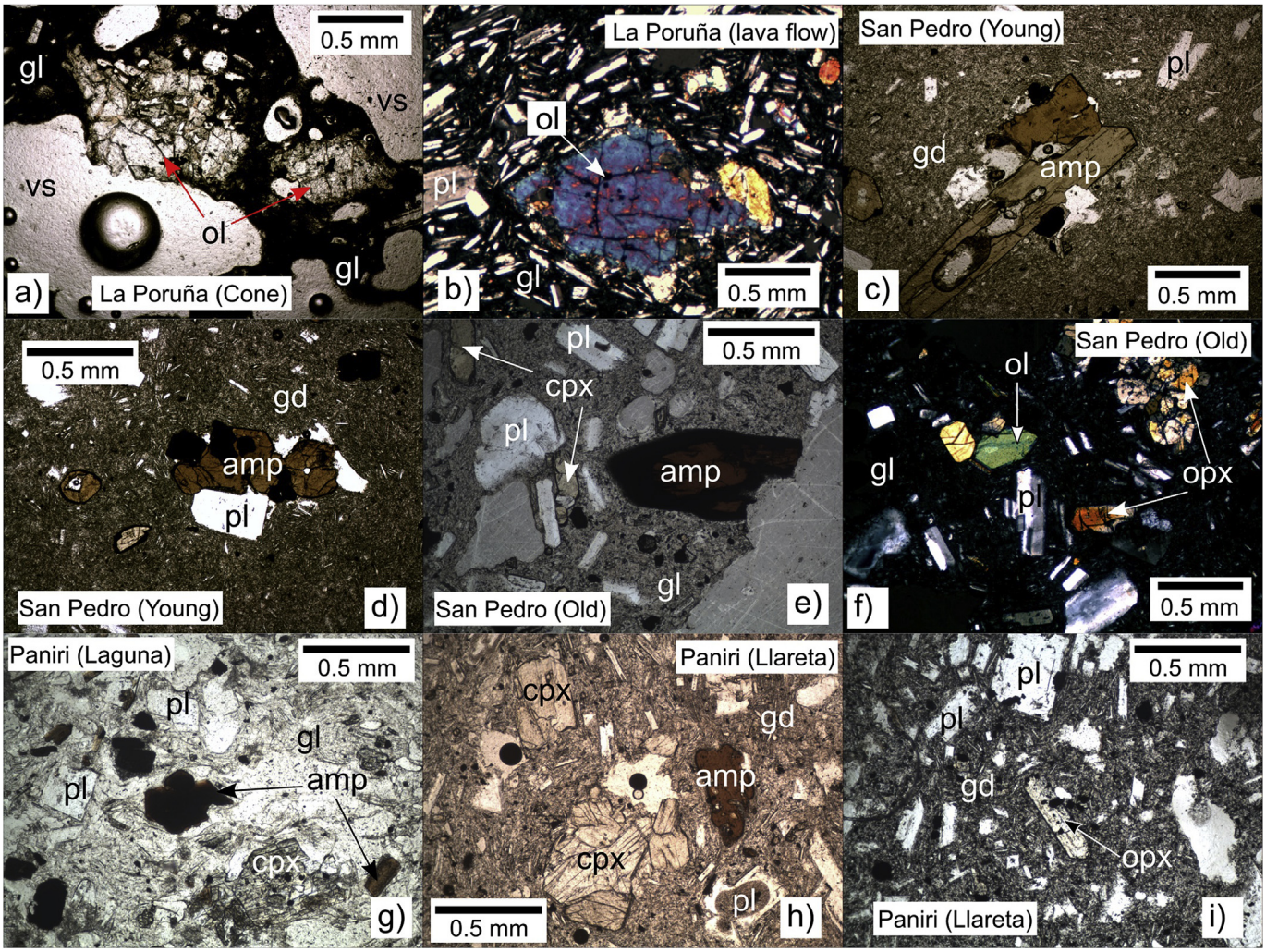

Fig. 3. Photomicrographis showing the main petrographic features of analyzed volcanic structures. Samples from the cone (a) and the lava flow (b) of La Poruña. Representative samples from Young (c–d), and Old (e–f) stages of San Pedro volcano (*sensu* González-Maurel et al., 2019a). Samples from Laguna (g) and Llareta (h–i) units of Paniri volcano (after Godoy et al., 2018). vs - vesicle; gl - glass; ol - olivine; pl - plagioclase; opx - orthopyroxene; gd - groundmass; amp - amphibole; cpx - clinopyroxene.

Their Sr isotopic compositions are close to mantle values (0.7039, McGee et al., 2019) with no correlation with indices of differentiation, suggesting little to no crustal contribution. These values are therefore representative of a mantle-dominated magmatic system, and this data could be extrapolated towards a fluid-enriched trend in ($^{238}U/^{232}Th$) vs ($^{230}Th/^{232}Th)_0$ (Fig. 4a). For El Misti, mantle-derived fluid addition has proposed to play a key role in its magmatic evolution (Kiebala, 2008), suggested by the proposed model for this volcanic structure (Fig. 4a). However, although we cannot rule out U-excess contributions from the mantle for the magmatic evolution of the San Pedro-Linzor volcanic chain, which could be higher than those for El Misti (Fig. 4a), we believe these are later largely overprinted by crustal processes, as we now discuss. The less evolved analyzed samples of the San Pedro-Linzor volcanic chain (i.e. La Poruña) have ^{238}U excess, and the highest Ba/Hf ratios of the volcanic chain. However, the obtained Ba/Hf ratios are lower than those from El Misti (Fig. 5a), and these ratios do not correlate with ($^{238}U/^{230}Th)_0$ (Fig. 5b), as expected if fluids are related to ^{238}U enrichment (McGee et al., 2019). Similar characteristics are observed for K/La ratios, which are lower than those from El Misti and do not correlate with ($^{238}U/^{230}Th)_0$ (Fig. 5c and d). Moreover, the increase in ^{238}U from La Poruña to Paniri is not correlated with the increasing of mantle hydration by slab-derived fluids in the same direction (Rosner et al., 2003) (Fig. 4b). This indicates that, even though fluid addition can be responsible for an initial ^{238}U excess, as observed for La Poruña, this is not the main process controlling this isotopic enrichment for the volcanic chain, as usually suggested for subduction-related volcanism (e.g. Turner et al., 2003; Garrison et al., 2006; Kiebala, 2008; Brens Jr., 2011; Huang et al., 2017; McGee et al., 2019).

^{238}U excess can also be generated by in-growth melting processes in the mantle, which is generated by melting of a low porosity matrix (i.e. mantle-wedge) (Huang et al., 2011). This process occurs in an oxidized mantle wedge, as higher oxygen fugacity causes a decrease in $D_{U/Th}$ from > 1 to < 1 (Huang et al., 2011). Grocke et al. (2016) indicated that high oxygen fugacity exists for magmas erupted in the Central Andes, based on the iron geochemical characteristics of the analyzed lavas. These authors suggested that the oxygen fugacity at this volcanic arc is associated with primary slab/mantle melting processes rather than a crustal control. Moreover, the oxygen fugacity is proposed to be higher near the trench, decreasing towards the back arc (Grocke et al., 2016). As observed, the ^{238}U excess increases eastwards for the San Pedro-Linzor volcanic chain (Fig. 4b) which is opposite to the increasing oxygen fugacity trend proposed for the Central Andean volcanic arc (Grocke et al., 2016). Thus, variations in ^{238}U excess are not associated with mantle in-growth below the San Pedro-Linzor volcanic chain.

Within other magmatic systems in the Andes, ^{238}U depletion (i.e.

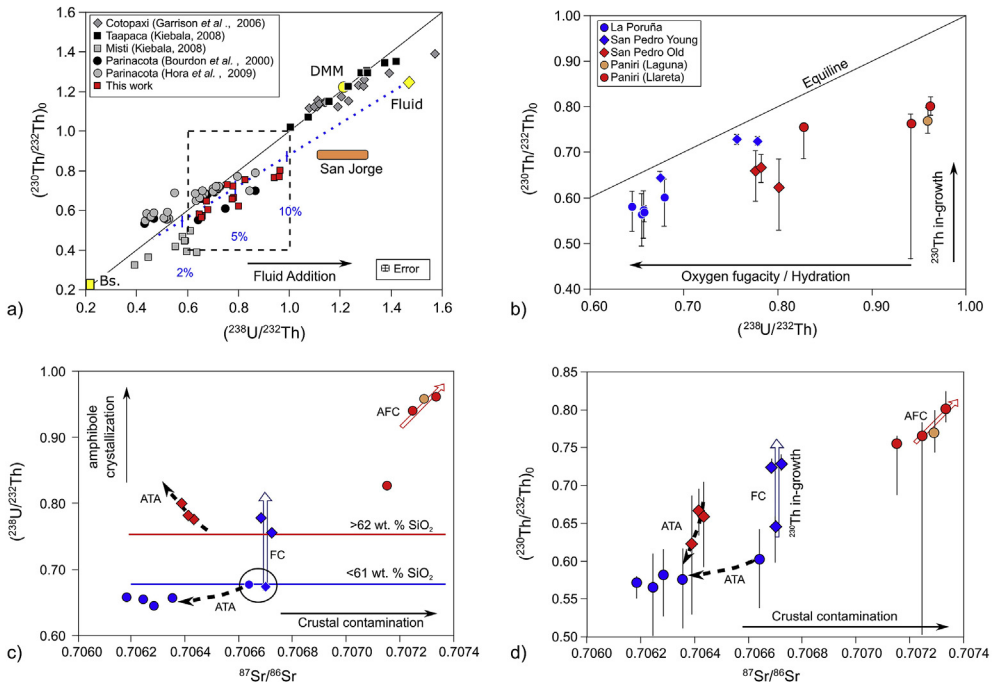

Fig. 4. $(^{230}Th/^{232}Th)_0$ *versus* $(^{238}U/^{232}Th)$ diagram, for Andean volcanoes (a), and for the analyzed lavas from San Pedro-Linzor volcanic chain (b) with equiline and error bars. $(^{238}U/^{232}Th)$ (c), and $(^{230}Th/^{232}Th)_0$ (d) *versus* $^{87}Sr/^{86}Sr$ ratios. In (c) the increase of $(^{238}U/^{232}Th)$ with differentiation is observed. Differentiation processes associated with assimilation and fractional crystallization (AFC), fractional crystallization (FC), and assimilation during turbulent ascent (ATA) (after Godoy et al., 2018, and González-Maurel et al., 2019a) are indicated with symbols as Fig. 1, see discussion. Star indicates the youngest erupted product of Paniri volcano. For (c) symbols include associated error. In a) model from Kiebala (2008) which considers data from Paleozic Basement (Bs.), Depleted MORB Mantle (DMM), and Fluids is included. Orange rectangle represents data from San Jorge (McGee et al., 2019). Arrow which indicates increasing fluid addition after Garrison et al. (2006) and Kiebala (2008). Errors bars for $(^{230}Th/^{232}Th)_0$ of this study consider analytical error and the error associated to the maximum and minimum age of each sample (see Table S4). In (b) arrows related to Th in-growth (Peate and Hawkesworth, 2005), and increasing mantle hydration (Rosner et al., 2003) and oxygen fugacity (Grocke et al., 2016) at Central Andes are included. (For interpretation of the references to colour in this figure legend, the reader is referred to the Web version of this article.)

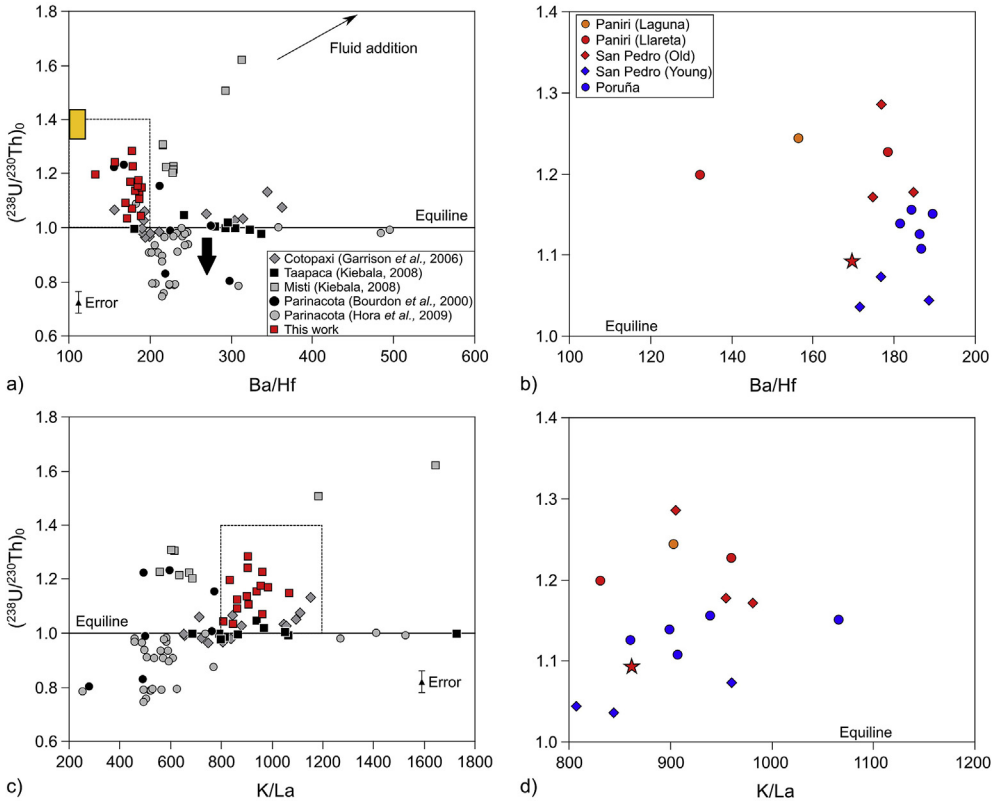

Fig. 5. $(^{238}U/^{230}Th)_0$ *versus* Ba/Hf diagram for Andean volcanoes (a), and for the analyzed lavas from San Pedro-Linzor volcanic chain (b). In (a) fluid addition arrow according to models from Bourdon et al. (2000) and Kiebala (2008). Thick black arrow indicates melting with garnet (after Bourdon et al., 2000). Orange rectangle area according to data from San Jorge (McGee et al., 2019). $(^{238}U/^{230}Th)_0$ *versus* K/La diagram for Andean volcanoes (c), and for the analyzed lavas from San Pedro-Linzor volcanic chain (d). $(^{238}U/^{230}Th)_0$ shows no systematic correlation with fluid mobile ratios for the volcanic chain. In (b) and (d), star indicates the youngest erupted product of Paniri volcano, and symbols include error. For (a) and (c), maximum error is shown (after Hora et al., 2009). Trace element data for Cotopaxi and Parinacota after Garrison et al. (2011), and Mamani et al. (2010), respectively. (For interpretation of the references to colour in this figure legend, the reader is referred to the Web version of this article.)

^{230}Th enrichment), and high LREE/HREE ratios have been related to garnet fractionation at lower levels in the thick crust (Garrison et al., 2006; Hora et al., 2009; Mamani et al., 2010). As the analyzed lavas show ^{238}U enrichment (Fig. 4b), no involvement of garnet fractionation is suggested in the evolution of the San Pedro-Linzor volcanic chain, which has also been proposed for other products of the main arc at the Altiplano-Puna Volcanic Complex using LREE/HREE ratios (Godoy et al., 2019).

Given the lack of correlation between fluid mobile/immobile elements and $(^{238}U/^{232}Th)$, we suggest that the U-series disequilibria in the San Pedro-Linzor lavas is mostly controlled by processes associated with magmatic differentiation rather than by the source, which occurs

mainly at upper-crustal levels (i.e. Shallow-MASH; Godoy et al., 2014, 2019; González-Maurel et al., 2020). Data falling near or on the equiline is associated with stagnation of magmas > 350 kyr (Bourdon et al., 2000; Kiebala, 2008) (Fig. 4a). The observed disequilibria (Figs. 4 and 5) for the volcanic chain suggest that these upper crustal magmatic processes occurred in the last 350 kyr, as indicated for other Andean volcanoes (e.g. Bourdon et al., 2000; Garrison et al., 2006; Kiebala, 2008). Thus, the main differentiation processes established for the volcanic chain (i.e. FC, AFC, and ATA; Fig. 2) are used here to constrain the evolution of U-series disequilibria in the last 350 kyr.

5.1.1. The role of amphibole fractionation

The different trends observed for ($^{238}U/^{232}Th$) with evolution of San Pedro Young and La Poruña (Fig. 4) suggests that ($^{238}U/^{232}Th$) variations are related to upper crustal differentiation processes in which a mineralogical phase fractionates when silica content increases over 62 wt%. Garrison et al. (2006) described the presence of allanite and apatite in rhyolitic lavas sampled from Cotopaxi (Northern Andes, Ecuador). These authors related the U-enrichment of these lavas to fractionation of Th-retaining mineralogical phases from an andesitic parental magma at upper crustal levels. However, allanite was not observed in previous descriptions of the San Pedro-Linzor volcanic chain (Godoy et al., 2017, 2018; González-Maurel et al., 2019a) nor the analyzed samples here (Fig. 3). Petrographically, apatite was recognized as an accessory mineral phase in some of the most evolved lavas from Paniri (Martínez, 2014; Godoy et al., 2018), however it was not recognized in the analyzed samples (Fig. 3). Apatite was also not recognized in lavas from La Poruña, but it is inferred to be present during differentiation of magmas from this volcanic structure by an inverse correlation between P_2O_5 (wt. %) and SiO_2 as index of differentiation (González-Maurel et al., 2019a) (Fig. 6a). However, ($^{238}U/^{232}Th$) in La Poruña decreases with differentiation (Fig. 4), which is not consistent with fractionation of a Th-retaining mineral from the residual melt generated during magmatic evolution of this volcanic structure. Also, there is no correlation between P_2O_5 (wt. %) and ($^{238}U/^{232}Th$) (Fig. 6b). Therefore we discard the role of allanite and apatite in the control of the observed ^{238}U enrichment of the analyzed samples.

Garrison et al. (2006) suggested that ^{238}U excess can be generated by assimilation of an amphibole-bearing crust. At the Altiplano-Puna Volcanic Complex, amphibole is an important mineralogical phase (i.e. O'Callaghan and Francis, 1986; Feeley and Davidson, 1994; Burns et al., 2015; Gorini et al., 2018), which fractionates at depths < 25 km (Feeley and Davidson, 1994; Matthews et al., 1994; Burns et al., 2015; Gorini et al., 2018) and can be associated with the evolution of the Altiplano-Puna Magma Body (Burns et al., 2015; Gorini et al., 2018). This is also recognized at the San Pedro-Linzor volcanic chain, where amphibole is an important mineral phase mainly in lavas with SiO_2 content > 62 wt% (O'Callaghan and Francis, 1986; Godoy et al., 2018; González-Maurel et al., 2019a). This phase (Fig. 3), is related to the decrease of CaO + Al_2O_3 (wt. %; Fig. 6c) and Dy/Dy* (after Davidson et al., 2013) with differentiation (Fig. 7a). Thus, the relationship between decreasing CaO + Al_2O_3 (wt. %) and Dy/Dy* with increasing ($^{238}U/^{232}Th$) (Figs. 6d and 7b) suggests that the ^{238}U excess can be related to amphibole crystallization, as this phase retains Th during differentiation (e.g. Berlo et al., 2004; Jicha et al., 2005; Garrison et al., 2006; Huang et al., 2008; Hora et al., 2009). Therefore, although partition coefficients for amphibole for U and Th are < 1, the bulk $D_{U/Th}$ ratio for this mineral (< 1) and the importance of this mineralogical phase in the magmatic evolution of the Central Andes suggest that amphibole crystallization is responsible for the relatively high ($^{238}U/^{232}Th$) ratios recognized during evolution of San Pedro (Young and Old) and Paniri lavas.

($^{230}Th/^{232}Th)_0$ ratios for San Pedro Young are substantially higher than for San Pedro Old (Fig. 7c), which is significant compared to the other analyzed volcanic suites with old and young phases (Figs. 3d and 7c). ^{230}Th in-growth by radioactive decay of ^{238}U has been related to an increase of ($^{230}Th/^{232}Th)_0$ in magmas during stagnation in shallow chambers (Condomines et al., 2003; Peate and Hawkesworth, 2005). Thus, we propose that the negative correlation of ($^{230}Th/^{232}Th)_0$ with Dy/Dy* (Fig. 7c) for lavas of San Pedro Young is indicative of ^{230}Th in-growth during FC differentiation from olivine-pyroxene-bearing to

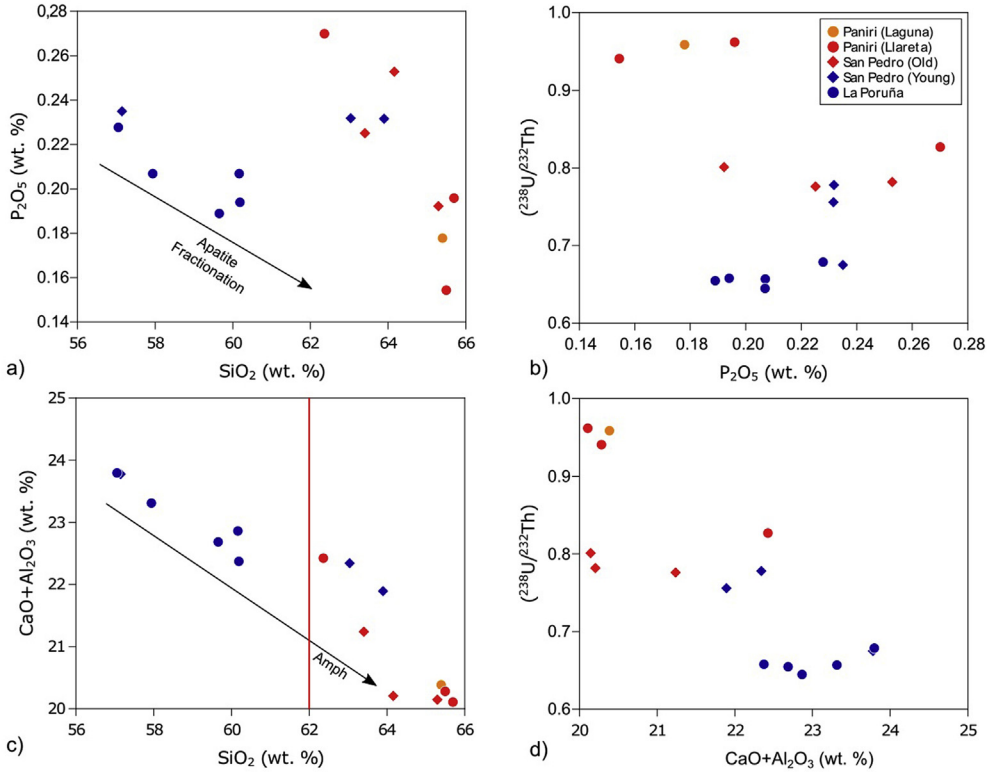

Fig. 6. a) P_2O_5 (wt. %) vs. SiO_2 (wt. %); b) ($^{238}U/^{232}Th$) vs. P_2O_5 (wt. %); c) CaO + Al_2O_3 (wt. %) vs. SiO2 (wt. %); and d) ($^{238}U/^{232}Th$) vs. CaO + Al_2O_3 (wt. %) diagrams for the analyzed samples. In a) a decrease in P_2O_5 content with differentiation is recognized for La Poruña, which is associated with apatite fractionation. In b) no strong correlation is observed between apatite and ^{238}U excess related to Th fractionation. In c) a decrease of CaO + Al_2O_3 (wt. %) with differentiation is observed in all the sample suites, which is associated with amphibole fractionation that occurs at lavas with SiO_2 > 62 (wt. %). In d) an inverse correlation is observed between CaO + Al_2O_3 (wt. %) and ($^{238}U/^{232}Th$).

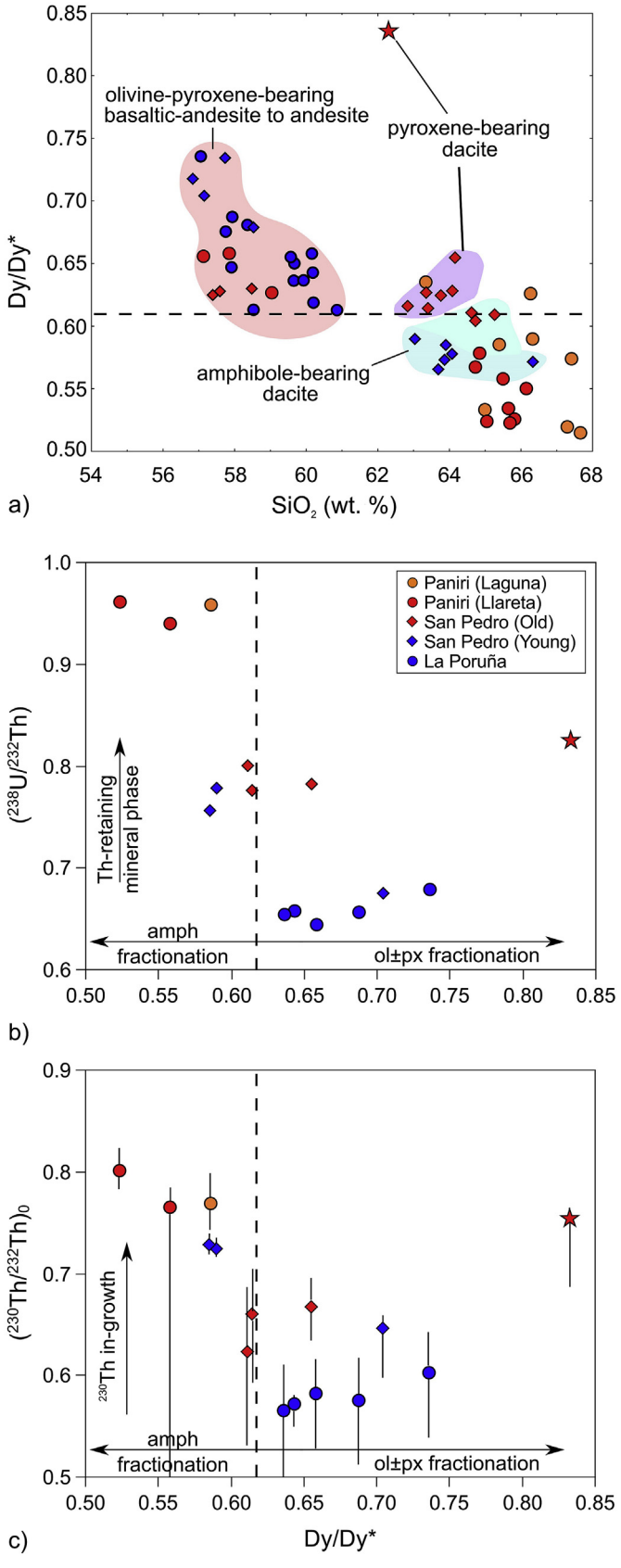

Fig. 7. Dy/Dy* (after Davidson et al., 2013) *versus* SiO_2 (wt. %) (a), and ($^{238}U/^{232}Th$) (b), and ($^{230}Th/^{232}Th)_0$ (c) *versus* Dy/Dy* diagrams for the analyzed volcanic structures. In (a) Dy/Dy* decreases with differentiation, and amphibole content. Fields after González-Maurel et al. (2019a). In b) and c) the U-Th activity ratios increase with the decreasing amphibole fractionation in the samples. Star indicates the youngest erupted product of Paniri volcano. Dashed lines indicate start of amphibole fractionation. In b) symbols include error.

amphibole-bearing suites within shallow crustal magmatic chambers (González-Maurel et al., 2019a). This also is plausible for the more evolved lavas of Paniri volcano, although to a lesser extent (Fig. 7c).

5.1.2. The role of crustal contamination and mafic inputs

Except for San Pedro Young, all suites show a positive correlation between ($^{230}Th/^{232}Th)_0$ and $^{87}Sr/^{86}Sr$ (Fig. 3d). This indicates that both ratios are mainly associated with crustal contamination (e.g. Huang et al., 2008), which is an important process at San Pedro-Linzor volcanic chain (Godoy et al., 2017, 2018; González-Maurel et al., 2019a,b; 2020), and the Central Andes (e.g. Davidson et al., 1990; Feeley et al., 1993; Matthews et al., 1994; Taussi et al., 2019). This contamination is related to differentiation processes occurring due to magma stagnation during which ^{230}Th in-growth is generated (Fig. 7c). Thus, the most evolved, and least contaminated (Fig. 2a), products of La Poruña and San Pedro Old show low ($^{230}Th/^{232}Th)_0$ (Fig. 4c). This highlights the ATA processes proposed for these volcanic structures, on which contamination (indicated by $^{87}Sr/^{86}Sr$ and ($^{230}Th/^{232}Th)_0$) decreases with the increasing silica content of the magmas (González-Maurel et al., 2019a,b). Jicha et al. (2005) proposed that abrupt shifts in magmatic evolution toward successively lower ($^{230}Th/^{232}Th)_0$ reflect the influx of magma into the system or the mixing of newly arrived magma with melt that remained in the deep reservoir. Thus, the lowest ($^{230}Th/^{232}Th)_0$ obtained for the youngest product of Paniri (Figs. 4d and 7c) indicates a magmatic recharge occurring in the related magmatic system, as these recharging magmas would have $^{87}Sr/^{86}Sr$ ratios < 0.706 in the Central Andes (Burns et al., 2015, 2020; Godoy et al., 2017; de Silva and Kay, 2018).

5.1.3. Upper crustal evolution and ^{238}U-^{230}Th systematics at San Pedro-Linzor volcanic chain

The obtained ^{238}U-^{230}Th data for the San Pedro-Linzor volcanic chain allows us to re-evaluate the existing ideas on magma genesis in the volcanic chain, and the Altiplano-Puna Volcanic Complex. Thus, we propose that the ($^{238}U/^{232}Th$) observed for analyzed products older than 100 ka (i.e. San Pedro Old and Paniri) are related to assimilation of an upper crustal source that mainly fractionated plagioclase + amphibole ± pyroxene, as indicated by Godoy et al. (2018) and González-Maurel et al. (2019a) (Fig. 8). For San Pedro Old, ATA differentiation generates an increase of amphibole fractionation with decreasing Sr-isotope content of the lavas (González-Maurel et al., 2019a), which leads to the negative correlation between ($^{238}U/^{232}Th$) with $^{87}Sr/^{86}Sr$ (Fig. 4c), and Dy/Dy* (Fig. 7b). However, as no significant stagnation of magmas occurs, ^{230}Th in-growth is not developed (Fig. 7c). Evolution of Paniri by AFC increases ($^{238}U/^{232}Th$), ($^{230}Th/^{232}Th)_0$, and $^{87}Sr/^{86}Sr$ with differentiation (Fig. 4c–d), during which amphibole fractionation occurred. After this stage, a change in the dominant mineralogy of the system is proposed for the products that were erupted in the last 100 kyr (González-Maurel et al., 2019a) (Fig. 8). This change involves fractionation of plagioclase + olivine + pyroxene in the less evolved magmas (Godoy et al., 2018; González-Maurel et al., 2019a), which decreases the ($^{238}U/^{232}Th$) of La Poruña, and the less-evolved products of San Pedro Young and Paniri (Figs. 3c and 7b). The decrease in ($^{230}Th/^{232}Th)_0$ with $^{87}Sr/^{86}Sr$ in the youngest volcanic product of Paniri (Fig. 4d) suggest that the mineralogical change is due to new mafic injections from a deeper source (Fig. 8) (e.g. Burns et al., 2020), which also progressively lowers the initial $^{87}Sr/^{86}Sr$ and ($^{230}Th/^{232}Th)_0$ of the

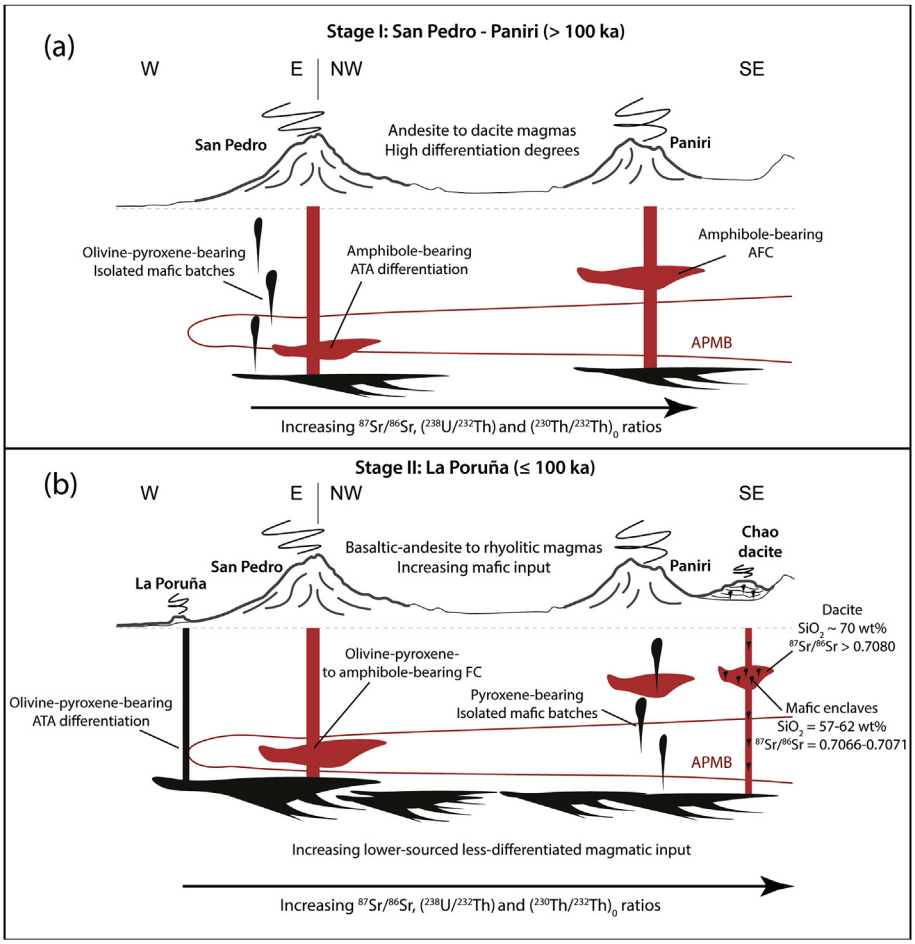

Fig. 8. Schematic evolution (not to scale) of the San Pedro-Linzor volcanic chain (after González-Maurel et al., 2019a). This evolution is related to interaction of mantle-derived magmas with a felsic upper crustal partially molten layer, which increases eastwards (Godoy et al., 2017). Initially (a) an amphibole-bearing fractionation dominates the upper crustal magmatic differentiation. This differentiation is associated mainly with assimilation during turbulent ascent (ATA) and assimilation and fractional crystallization (AFC) processes. In the last 100 ka (b), a lowering of the ($^{238}U/^{232}Th$) by changing the main mineralogical assemblage is recognized. Changes in the initial $(^{230}Th/^{232}Th)_0$ of the suites are associated with an increase in the mafic input, which increases crustal contamination (González-Maurel et al., 2019a). ^{230}Th in-growth in this stage is due to fractional crystallization (FC) which generates amphibole-bearing assemblages (i.e. San Pedro Young). For La Poruña, San Pedro, and Paniri, data from Godoy et al. (2018), and González-Maurel et al. (2019a). Data for Chao Dacite from de Silva et al. (1994). Composition of mafic enclaves after Taussi et al. (2019).

analyzed volcanic structures with time (González-Maurel et al., 2019a). The development of shallow (4–8 km depth) magmatic chambers below San Pedro volcano allows FC evolution during which amphibole crystallizes, which causes ^{238}U decay and ^{230}Th in-growth. We suggest that this new mafic input could trigger the eruption of the nearby Chao Dacite and Chillahuita domes (Figs. 1 and 8) of ca. 100 ka (Tierney et al., 2016), which are coeval with La Poruña, the first stages of San Pedro Young and the youngest event of Paniri. Mafic input as a possible eruption trigger is proposed for other enclave-hosting domes of the Central Andes (e.g. Watts et al., 1999; Taussi et al., 2019; Godoy et al., 2019; Burns et al., 2020).

6. Conclusions

To completely understand the U-series disequilibria signatures of a particular magmatic system it is important to establish its origin and evolution using a combination of detailed whole-rock geochemistry (e.g. major oxide, trace and rare earth elements, and Sr and Nd radiogenic isotopes), and geochronological and stratigraphic information. The U-series characteristics of the San Pedro-Linzor volcanic chain are mostly related to the upper crustal evolution of subduction-related mantle-derived magmas, previously defined using detailed geological, geochemical and radiogenic isotope characteristics. The U-series isotopic signature therefore recorded: i) the different degrees of interaction of mantle-derived magmas with partially molten upper crustal layers, ii) the differentiation processes during ascent to the surface, and iii) new mantle-derived mafic injections. This shows that ^{238}U and ^{230}Th changes in this volcanic chain in the Central Andes are related to magmatic evolution at upper crustal levels. U-series systematics in this, and similar complex tectonic environments, is therefore not necessarily dominated by fluid addition into the mantle wedge.

Author statement

Benigno Godoy - Conceptualization, Investigation, Visualization, Formal Analysis, Methodology, Resources, Writing - Original Draft, Writing - Review and Editing, Funding Acquisition. Lucy McGee - Investigation, Resources, Visualization, Writing - Original Draft, Writing - Review and Editing. Petrus le Roux - Investigation, Resources, Writing - Original Draft, Writing - Review and Editing. Osvaldo González-Maurel - Formal Analysis, Resources, Visualization, Writing - Original Draft, Writing - Review and Editing, Funding Acquisition. Inés Rodríguez - Writing - Original Draft, Writing - Review and Editing. Diego Morata - Writing - Original Draft, Writing - Review and Editing, Funding Acquisition. Andrew Menzies - Writing - Original Draft, Writing - Review and Editing.

Declaration of competing interest

The authors declare that they have no known competing financial interests or personal relationships that could have appeared to influence the work reported in this paper.

Acknowledgments

This work was funded by the Comisión Nacional de Investigación Científica y Tecnológica [FONDECYT PostDoctorado Nº 3160432 to B.G; CONICYT-PCHA/Doctorado Nacional/2015–21150403 to O.G.-M.], and Centro de Excelencia en Geotermia de los Andes- Universidad de Chile [FONDAP-CONICYT 15090013]. We also thank Dr. Andrés

Folguera and an anonymous reviewer for fruitful comments made to improve this manuscript. We also thank Dr. Dennis Brown and two anonymous reviewers for helpful comments in previous versions of this manuscript.

Appendix A. Supplementary data

Supplementary data to this article can be found online at https://doi.org/10.1016/j.jsames.2020.102672.

References

Araya Vargas, J., Meqbel, N.M., Ritter, O., Brasse, H., Weckmann, U., Yáñez, G., Godoy, B., 2019. Fluid distribution in the Central Andes subduction zone imaged with magnetotellurics. J. Geophys. Res.: Solid Earth 124 (4), 4017–4043. https://doi.org/10.1029/2018JB016933.

Beck, S.L., Zandt, G., Myers, S.C., Wallace, T.C., Silver, P.G., Drake, L., 1996. Crustal-thickness variations in the central Andes. Geology 24 (5), 407–410. https://doi.org/10.1130/0091-7613(1996)024%3C0407:CTVITC%3E2.3.CO;2.

Berlo, K., Turner, S., Blundy, J., Hawkesworth, C., 2004. The extent of U-series disequilibria produced during partial melting of the lower crust with implications for the formation of the Mount St. Helens dacites. Contrib. Mineral. Petrol. 148 (1), 122–130. https://doi.org/10.1007/s00410-004-0590-2.

Bertín, D., Amigo, A., 2019. Geología del Volcán San Pedro, Región de Antofagasta. Servicio Nacional de Geología y Minería, Carta Geológica de Chile, Serie Geología Básica, No. pp. 1 mapa escala 1:50.000. Santiago, Chile.

Bourdon, B., Wörner, G., Zindler, A., 2000. U-series evidence for crustal involvement and magma residence times in the petrogenesis of Parinacota volcano, Chile. Contrib. Mineral. Petrol. 139 (4), 458–469. https://doi.org/10.1007/s004100000150.

Brens Jr., R., 2011. U-Th-Ba Elemental Fractionation during Partial Melting of Crustal Xenoliths and its Implications for U-Series Disequilibria in Continental Arc Rocks. [M.Sc. thesis]. Florida International University, USA, pp. 102. https://doi.org/10.25148/etd.FI11052301.

Burns, D.H., de Silva, S.L., Tepley III, F., Schmitt, A.K., Loewen, M.W., 2015. Recording the transition from Flare-up to Steady-state arc magmatism at the Purico–Chascon volcanic complex, northern Chile. Earth Planet Sci. Lett. 422, 75–86. https://doi.org/10.1016/j.epsl.2015.04.002.

Burns, D.H., de Silva, S.L., Tepley, F.J., Schmitt, A.K., 2020. Chasing the mantle: deciphering cryptic mantle signals through Earth's thickest continental magmatic arc. Earth Planet Sci. Lett. 531, 115985. https://doi.org/10.1016/j.epsl.2019.115985.

Chmielowski, J., Zandt, G., Haberland, C., 1999. The central Andean Altiplano-Puna magma body. Geophys. Res. Lett. 26 (6), 783–786. https://doi.org/10.1029/1999GL900078.

Condomines, M., Gauthier, P.-J., Sigmarsson, O., 2003. Timescales of magma chamber processes and dating of young volcanic rocks. In: In: Bourdon, B., Henderson, G.M., Lundstrom, C.C., Turner, S.P. (Eds.), Uranium-series Geochemistry, *Reviews in Mineralogy and Geochemistry*, vol. 52. pp. 25–174. https://doi.org/10.2113/0520125. 1.

Davidson, J.P., McMillan, N.J., Moorbath, S., Wörner, G., Harmon, R.S., López-Escobar, L., 1990. The Nevados de Payachata volcanic region (18°S/69°W, N. Chile) II. Evidence for widespread crustal involvement in Andean magmatism. Contrib. Mineral. Petrol. 105, 412–432. https://doi.org/10.1007/BF00286829.

Davidson, J.P., Harmon, R.S., Wörner, G., 1991. The source of central Andean magmas: some considerations. In: In: Harmon, R.S., Rapela, C.W. (Eds.), Andean Magmatism and its Tectonic Setting, vol. 265. Geological Society of America Special Paper, pp. 233–243. https://doi.org/10.1130/SPE265-p233.

Davidson, J., Turner, S., Plank, T., 2013. Dy/Dy*: variations arising from mantle sources and petrogenetic processes. J. Petrol. 54 (3), 525–537. https://doi.org/10.1093/petrology/egs076.

de Silva, S.L., 1989. Altiplano-Puna volcanic complex of the central Andes. Geology 17 (12), 1102–1106. https://doi.org/10.1130/0091-7613.

de Silva, S.L., Kay, S.M., 2018. Turning up the heat: high-flux magmatism in the central Andes. Elements 14 (4), 245–250. https://doi.org/10.2138/gselements.14.4.245.

de Silva, S.L., Self, S., Francis, P.W., Drake, R.E., Ramírez, C., 1994. Effusive silicic volcanism in the Central Andes: the Chao dacite and other young lavas of the Altiplano-Puna volcanic complex. J. Geophys. Res. 99 (B9), 17805. https://doi.org/10.1029/94JB00652.

de Silva, S.L., Zandt, G., Trumbull, R., Viramonte, J.G., Salas, G., Jiménez, N., 2006. Large ignimbrite eruptions and volcano-tectonic depressions in the Central Andes: a thermomechanical perspective. Geol. Soc. Lond. Spec. Publ. 269, 47–63. https://doi.org/10.1144/GSL.SP.2006.269.01.04.

Delunel, R., Blard, P.H., Martin, L.C.P., Nomade, S., Schlunegger, F., 2016. Long term low latitude and high elevation cosmogenic 3He production rate inferred from a 107 ka-old lava flow in northern Chile; 22°S-3400 m a.s.l. Geochem. Cosmochim. Acta 184, 71–87. https://doi.org/10.1016/j.gca.2016.04.023.

DePaolo, D.J., 1981. Trace element and isotopic effects of combined wallrock assimilation and fractional crystallization. Earth Planet Sci. Lett. 53 (2), 189–202. https://doi.org/10.1016/0012-821X(81)90153-9.

Feeley, T.C., Davidson, J.P., 1994. Petrology of calc-alkaline lavas at Volcán Ollagüe and the origin of compositional diversity at Central Andean stratovolcanoes. J. Petrol. 35 (5), 1295–1340. https://doi.org/10.1093/petrology/35.5.1295.

Feeley, T.C., Davidson, J.P., Armendia, A., 1993. The volcanic and magmatic evolution of Volcán Ollagüe, a high-K, late quaternary stratovolcano in the Andean Central Volcanic Zone. J. Volcanol. Geoth. Res. 54 (3–4), 221–245. https://doi.org/10.1016/0377-0273(93)90065-Y.

Figueroa, J., Figueroa, O., 2006. Petrografía y geoquímica de las lavas del volcán Sairecabur, Andes Centrales, Chile. In: Actas, vol. 2. XI Congreso Geológico Chileno, Antofagasta, Chile, pp. 459–462.

Francis, P.W., Roobol, M.J., Walker, G.P.L., Cobbold, P.R., Coward, M., 1974. The San Pedro and San Pablo volcanoes of northern Chile and their hot avalanche deposits. Geol. Rundsch. 63 (1), 357–388. https://doi.org/10.1007/BF01820994.

Gallmeyer, G., 2018. Petrología de los enclaves máficos en domos dacíticos y su relación con el cono de escoria La Poruña, en la Cadena Volcánica San Pedro – Linzor, Andes Centrales, Chile. Dissertation, Bachelor's Degree Thesis. Universidad Católica del Norte, Antofagasta, Chile.

Garrison, J., Davidson, J., Reid, M., Turner, S., 2006. Source *versus* differentiation controls on U-series disequilibria: insights from Cotopaxi volcano, Ecuador. Earth Planet Sci. Lett. 244 (3–4), 548–565. https://doi.org/10.1016/j.epsl.2006.02.013.

Garrison, J., Davidson, J.P., Hall, M., Mothes, P., 2011. Geochemistry and petrology of the most recent deposits from Cotopaxi volcano, Northern Volcanic Zone, Ecuador. J. Petrol. 52 (9), 1641–1678. https://doi.org/10.1093/petrology/egr023.

Giambiagi, L., Alvarez, P., Spagnotto, S., 2015. Temporal variation of the stress field during the construction of the central Andes: constrains from the volcanic arc region (22–26°S), Western Cordillera, Chile, during the last 20 Ma. Tectonics 35 (9), 2014–2033. https://doi.org/10.1002/2016TC004201.

Godoy, B., Wörner, G., Kojima, S., Aguilera, F., Simon, K., Hartmann, G., 2014. Low-pressure evolution of arc magmas in thickened crust: the San Pedro-Linzor volcanic chain, Central Andes, Northern Chile. J. S. Am. Earth Sci. 52, 24–42. https://doi.org/10.1016/j.jsames.2014.02.004.

Godoy, B., Wörner, G., Le Roux, P., de Silva, S., Parada, M.A., Kojima, S., González-Maurel, O., Morata, D., Polanco, E., Martínez, P., 2017. Sr- and Nd- isotope variations along the pleistocene san Pedro – Linzor volcanic chain, N. Chile: tracking the influence of the upper crustal Altiplano-Puna magma body. J. Volcanol. Geoth. Res. 341, 172–186. https://doi.org/10.1016/j.jvolgeores.2017.05.030.

Godoy, B., Lazcano, J., Rodríguez, I., Martínez, P., Parada, M.A., le Roux, P., Wilke, H.-G., Polanco, E., 2018. Geological evolution of Paniri volcano, central Andes, northern Chile. J. S. Am. Earth Sci. 84, 184–200. https://doi.org/10.1016/j.jsames.2018.03.013.

Godoy, B., Taussi, M., González-Maurel, O., Renzulli, A., Hernández-Prat, L., le Roux, P., Morata, D., Menzies, A., 2019. Linking the mafic volcanism with the magmatic stages during the last 1 Ma in the main volcanic arc of the Altiplano-Puna Volcanic Complex (Central Andes). J. S. Am. Earth Sci. 95, 102295. https://doi.org/10.1016/j.jsames.2019.102295.

González-Maurel, O., Godoy, B., le Roux, P., Rodríguez, I., Marin, C., Menzies, A., Bertin, D., Morata, D., Vargas, M., 2019a. Magmatic differentiation at La Poruña scoria cone, Central Andes, northern Chile: evidence for assimilation during turbulent ascent processes, and genetic links with mafic eruptions at adjacent San Pedro volcano. Lithos 338–339, 128–140. https://doi.org/10.1016/j.lithos.2019.03.033.

González-Maurel, O., le Roux, P., Godoy, B., Troll, V.R., Deegan, F.M., Menzies, A., 2019b. The great escape: petrogenesis of low-silica volcanism of Pliocene to Quaternary age associated with the Altiplano-Puna Volcanic Complex of northern Chile (21°10'-22°50'S). Lithos 346–347, 105162. https://doi.org/10.1016/j.lithos.2019.105162.

González-Maurel, O., Deegan, F.M., le Roux, P., Harris, C., Troll, V.R., Godoy, B., 2020. Constraining the sub-arc, parental magma composition for the giant Altiplano-Puna Volcanic Complex, northern Chile. Sci. Rep. 10, 6864. https://doi.org/10.1038/s41598-020-63454-1.

Gorini, A., Ridolfi, F., Piscaglia, F., Taussi, M., Renzulli, A., 2018. Application and reliability of calcic amphibole thermobarometry as inferred from calc-alkaline products of active geothermal areas in the Andes. J. Volcanol. Geoth. Res. 358, 58–76. https://doi.org/10.1016/j.jvolgeores.2018.03.018.

Grocke, S.B., Cottrell, E., de Silva, S., Kelley, K.A., 2016. The role of crustal and eruptive processes versus source variations in controlling the oxidation state of iron in Central Andean magmas. Earth Planet Sci. Lett. 40, 92–104. https://doi.org/10.1016/j.epsl.2016.01.026.

Hawkesworth, C., Turner, S., Peate, D., McDermott, F., van Calsteren, P., 1997. Elemental U and Th variations in island arc rocks: implications for U-series isotopes. Chem. Geol. 139 (1–4), 207–221. https://doi.org/10.1016/S0009-2541(97)00036-3.

Hora, J.M., Singer, B.S., Wörner, G., Beard, B.L., Jicha, B.R., Johnson, C.M., 2009. Shallow and deep crustal control on differentiation of calc-alkaline and tholeiitic magma. Earth Planet Sci. Lett. 285 (1–2), 75–86. https://doi.org/10.1016/j.epsl.2009.05.042.

Huang, F., Gao, L., Lundstrom, C.C., 2008. The effect of assimilation, fractional crystallization, and ageing on U-series disequilibria in subduction zone lavas. Geochem. Cosmochim. Acta 72 (16), 4136–4145. https://doi.org/10.1016/j.gca.2008.05.060.

Huang, F., Lundstrom, C.C., Sigurdsson, H., Zhang, Z., 2011. U-series disequilibria in Kick'em Jenny submarine volcano lavas: a new view of time-scales of magmatism in convergent margins. Geochem. Cosmochim. Acta 75 (1), 195–212. https://doi.org/10.1016/j.gca.2010.05.036.

Huang, F., Xu, J., Zhang, J., 2016. U-series disequilibria in subduction zone lavas: inherited from subducted slabs or produced by mantle in-growth melting? Chem. Geol. 440, 179–190. https://doi.org/10.1016/j.chemgeo.2016.07.005.

Huang, F., Sørensen, E.V., Holm, P.M., Zhang, Z.-F., Lundstrom, C.C., 2017. U-series disequilibria of trachyandesites from minor volcanic centers in the Central Andes. Geochem. Cosmochim. Acta 215, 92–104. https://doi.org/10.1016/j.gca.2017.07.017.

Huppert, H.E., Sparks, R.S.J., 1985. Cooling and contamination of mafic and ultramafic magmas during ascent through continental crust. Earth Planet Sci. Lett. 74 (4),

371–386. https://doi.org/10.1016/S0012-821X(85)80009-15.
Jicha, B.R., Singer, B.S., Beard, B.L., Johnson, C.M., 2005. Contrasting timescales of crystallization and magma storage beneath the Aleutian Island arc. Earth Planet Sci. Lett. 236 (1–2), 195–210. https://doi.org/10.1016/j.epsl.2005.05.002.
Kern, J.M., de Silva, S.L., Schmitt, A.K., Kaiser, J.F., Iriarte, A.R., Economos, R., 2016. Geochronological imaging of an episodically constructed subvolcanic batholith: U-Pb in zircon chronochemistry of the Altiplano-Puna Volcanic Complex of the Central Andes. Geosphere 12 (4), 1–24. https://doi.org/10.1130/GES01258.1.
Kiebala, A., 2008. Magmatic Processes by U-Th Disequilibria Method. Comparison of Two Andean Systems: El Misti Volcano (S. Perú) and Taapaca Volcanic Center (N. Chile. Ph.D. thesis. University of Göttingen, Göttingen, Germany, pp. 94.
Kühn, C., Brasse, H., Schwarz, G., 2018. Three-dimensional electrical resistivity image of the volcanic arc in northern Chile - an appraisal of early magnetotelluric data. Pure Appl. Geophys. 175 (6), 2153–2165. https://doi.org/10.1007/s00024-017-1764-y.
Lazcano, J., 2016. Evolución volcanológica del Volcán Paniri (Región de Antofagasta, Chile). Dissertation, Bachelor's Degree Thesis. Universidad Católica del Norte, Antofagasta, Chile.
Mamani, M., Wörner, G., Sempere, T., 2010. Geochemical variations in igneous rocks of the Central Andean orocline (13°S to 18°S): tracking crustal thickening and magma generation through time and space. Geol. Soc. Am. Bull. 122 (1/2), 162–182. https://doi.org/10.1130/B26538.1.
Mancini, R., Díaz, D., Brasse, H., Godoy, B., Hernández, M.J., 2019. Conductivity distribution beneath the San Pedro-Linzor volcanic chain, North Chile, using 3D magnetotelluric modelling. J. Geophys. Res.: Solid Earth 124 (5), 4386–4398. https://doi.org/10.1029/2018JB016114.
Marín, C., 2016. Petrología del volcán La Poruña, Región de Antofagasta, Chile. Dissertation, Bachelor's Degree Thesis. Universidad Católica del Norte, Antofagasta, Chile.
Marín, C., Medina, E., Rodríguez, I., Pereira, M., 2015. Antecedentes petrográficos y geoquímicos del volcán La Poruña, región de Antofagasta, Chile. In: Actas XIV Congreso Geológico Chileno, La Serena, Chile, pp. 402–405.
Maro, G., Caffe, P.J., Romer, R.L., Trumbull, R.B., 2017. Neogene mafic magmatism in the northern Puna plateau, Argentina: generation and evolution of a back-arc volcanic suite. J. Petrol. 58 (8), 1591–1617. https://doi.org/10.1093/petrology/egx066.
Martínez, P., 2014. Petrología y geoquímica de lavas recientes, al noroeste del Campo Geotermal del Tatio. [B.Sc. thesis]. Universidad de Chile, Santiago, Chile, pp. 132.
Matthews, S.J., Jones, A.P., Gardeweg, M.C., 1994. Lascar volcano, northern Chile: evidence for steady-state disequilibrium. J. Petrol. 35 (2), 401–432. https://doi.org/10.1093/petrology/35.2.401.
McGee, L., Morgado, E., Brahm, R., Parada, M.-A., Vinet, N., Lara, L.E., Flores, A., Turner, M., Handley, H., Nowell, G., 2019. Stratigraphically controlled sampling captures the onset of highly fluid-fluxed melting at San Jorge volcano, Southern Volcanic Zone, Chile. Contrib. Mineral. Petrol. 174, 102. https://doi.org/10.1007/s00410-019-1643-x.
O'Callaghan, L.J., Francis, P.W., 1986. Volcanological and petrological evolution of san Pedro volcano, Provincia El Loa, North Chile. J. Geol. Soc. Lond. 143, 275–286. https://doi.org/10.1144/gsjgs.143.2.0275.
Peate, D.W., Hawkesworth, C.J., 2005. U series disequilibria: insights into mantle melting and the timescales of magma differentiation. Rev. Geophys. 43 (1), RG1003. https://doi.org/10.1029/2004RG000154.
Rogers, G., Hawkesworth, C.J., 1989. A geochemical traverse across the North Chilean Andes: evidence for crust generation from the mantle wedge. Earth Planet Sci. Lett. 91 (3–4), 271–285. https://doi.org/10.1016/0012-821X(89)90003-4.
Rosner, M., Erzinger, J., Franz, G., Trumbull, R.B., 2003. Slab-derived boron isotope signatures in arc volcanic rocks from the Central Andes and evidence for boron isotope fractionation during progressive slab dehydration. G-cubed 4 (8), 9005. https://doi.org/10.1029/2002GC000438.
Salfity, J.A., 1985. Lineamientos transversales al rumbo andino en el noroeste Argentino: IV Congreso Geológico Chileno, Antofagasta, Chile. Actas 2, 119–137.
Scott, S.R., Sims, K.W., Reagan, M.K., Ball, L., Schwieters, J.B., Bouman, C., Lloyd, N.S., Waters, C.L., Standish, J.J., Tollstrup, D.L., 2019. The application of abundance sensitivity filters to the precise and accurate measurement of uranium series nuclides by plasma mass spectrometry. Int. J. Mass Spectrom. 435, 321–332. https://doi.org/10.1016/j.ijms.2018.11.011.
Sellés, D., Gardeweg, M., 2017. Geología del área Ascotán-Cerro Inacaliri, Región de Antofagasta. Servicio Nacional de Geología y Minería, Carta Geológica de Chile. Serie Geología Básica 190 (73), 1 mapa escala 1:100.000. Santiago, Chile.
Taussi, M., Godoy, B., Piscaglia, F., Morata, D., Agostini, S., le Roux, P., González-Maurel, O., Gallmeyer, G., Menzies, A., Renzulli, A., 2019. The upper crustal magma plumbing system of the Pleistocene Apacheta-Aguilucho Volcanic Complex area (Altiplano-Puna, northern Chile) as inferred from the erupted lavas and their enclaves. J. Volcanol. Geoth. Res. 373, 179–198. https://doi.org/10.1016/j.jvolgeores.2019.01.021.
Tierney, C.R., Schmitt, A.K., Lovera, O.M., de Silva, S.L., 2016. Voluminous plutonism during volcanic quiescence revealed by thermochemical modeling of zircon. Geology 44 (8), 683–686. https://doi.org/10.1130/G37968.1.
Turner, S., Bourdon, B., Gill, J., 2003. Insights into magma genesis at convergent margins from U-series isotopes. In: In: Bourdon, B., Henderson, G.M., Lundstrom, C.C., Turner, S.P. (Eds.), Uranium-series Geochemistry, *Reviews in Mineralogy and Geochemistry*, vol. 52. pp. 255–315. https://doi.org/10.2113/0520255. 1.
Ward, K.M., Zandt, G., Beck, S.L., Christensen, D.H., McFarlin, H., 2014. Seismic imaging of the magmatic underpinnings beneath the Altiplano-Puna volcanic complex from the joint inversion of surface wave dispersion and receiver functions. Earth Planet Sci. Lett. 404, 43–53. https://doi.org/10.1016/j.epsl.2014.07.022.
Watts, R.B., de Silva, S.L., Jimenez de Rios, G., Croudace, I., 1999. Effusive eruption of viscous silicic magma triggered and driven by recharge: a case study of the Cerro Chascon-Tuntu Jarita Dome Complex in Southwest Bolivia. Bull. Volcanol. 60 (4), 241–264. https://doi.org/10.1007/s004450050274.
Wörner, G., Hammerschmidt, K., Henjes-Kunst, F., Lezaun, J., Wilke, H., 2000. Geochronology (40Ar/39Ar, K-Ar and He-exposure ages) of Cenozoic magmatic rocks from northern Chile (18 22°S): implications for magmatism and tectonic evolution of the central Andes. Rev. Geol. Chile 27 (2), 205–240. https://doi.org/10.4067/S0716-02082000000200004.